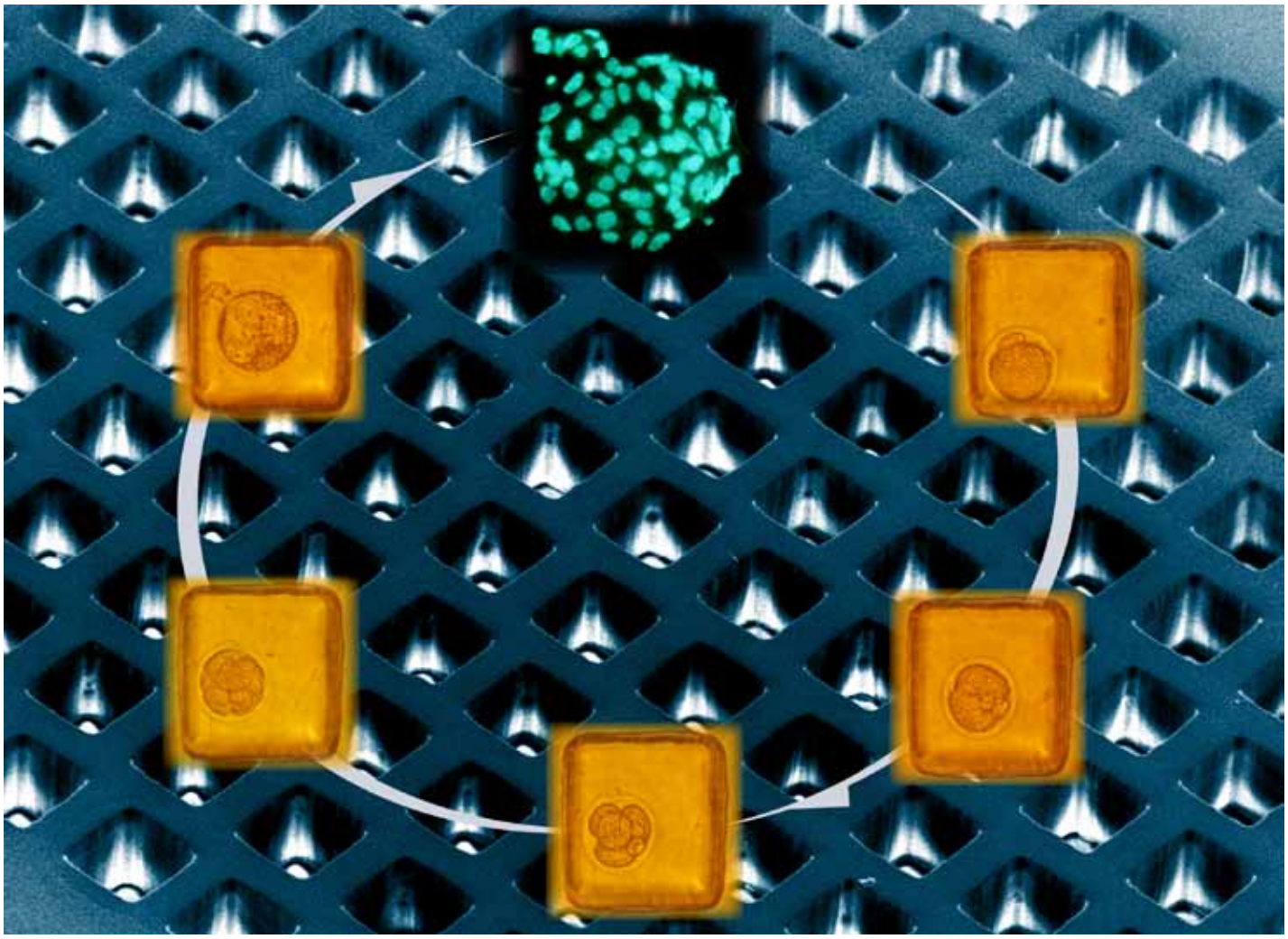

Featuring work performed in the Department of Biomedical Engineering of Dr Guoliang Huang at Tsinghua University, in collaboration with Dr Jie Qiao at the Center of Reproduction Medicine, Third Hospital of Peking University, Beijing, China.

Title: Integration of single oocyte trapping, *in vitro* fertilization and embryo culture in a microwell-structured microfluidic device

A novel microwell array structured microfluidic device integrates single murine oocyte trapping, fertilization and subsequent embryo culture, which may bring advantages to IVF practices by simplifying oocyte handling, allowing rapid medium changing, and enabling automated tracking of single embryo development.

As featured in:

See Huang and Qiao *et al.*, *Lab Chip*, 2010, **10**, 2848–2854.

Integration of single oocyte trapping, *in vitro* fertilization and embryo culture in a microwell-structured microfluidic device†‡

Chao Han,[ab] Qiufang Zhang,[c] Rui Ma,[ab] Lan Xie,[ab] Tian Qiu,[ab] Lei Wang,[b] Keith Mitchelson,[ab] Jundong Wang,[d] Guoliang Huang,*[ab] Jie Qiao*[c] and Jing Cheng[ab]

Received 5th May 2010, Accepted 23rd July 2010
DOI: 10.1039/c005296e

In vitro fertilization (IVF) therapy is an important treatment for human infertility. However, the methods for clinical IVF have only changed slightly over decades: culture medium is held in oil-covered drops in Petri dishes and manipulation occurs by manual pipetting. Here we report a novel microwell-structured microfluidic device that integrates single oocyte trapping, fertilization and subsequent embryo culture. A microwell array was used to capture and hold individual oocytes during the flow-through process of oocyte and sperm loading, medium substitution and debris cleaning. Different microwell depths were compared by computational modeling and flow washing experiments for their effectiveness in oocyte trapping and debris removal. Fertilization was achieved in the microfluidic devices with similar fertilization rates to standard oil-covered drops in Petri dishes. Embryos could be cultured to blastocyst stages in our devices with developmental status individually monitored and tracked. The results suggest that the microfluidic device may bring several advantages to IVF practices by simplifying oocyte handling and manipulation, allowing rapid and convenient medium changing, and enabling automated tracking of any single embryo development.

1 Introduction

Since the world's first test-tube baby was born in 1978,[1] assisted reproductive technology (ART) such as *in vitro* fertilization (IVF) has been used as an important therapy for the treatment of human infertility worldwide during the past three decades. The standard protocols for clinical IVF practice include gametes collection, fertilization and embryo culture, which remain nearly unchanged since its initiation, with culture medium held in oil-covered drops in Petri dishes, and manipulation performed manually by pipetting.[2] In these protocols, frequent pipetting of gametes is required, which is labor-intensive and time-consuming. In addition, fertilization and embryo culture require different media, therefore presumed zygotes have to be washed several times and transported to different drops for further development. Although some culture media have been developed to support both fertilization and embryo development (Complete Human Tubal Fluid (HTF) Medium with Serum Substitute Supplement (SSS), Irvine Scientific, Santa Ana, CA), the oocyte-washing step is still mandatory in order to remove the debris in the fertilization medium, which mainly consists of dead sperm. Another remaining issue is the ability to track the fertilization and development of an individual oocyte, since they are typically fertilized, washed, transferred and cultured in groups.

Microfluidic technology is an emerging field and has found increasing applications in recent years. In studies of assisted reproduction, microfluidics has the following unique advantages. The consumption of media in microfluidic devices is very low, thus only a small amount of sperm sample is needed to reach the same concentration as on a macro-scale.[3] Fluid in microchannels can be precisely predicted and controlled, allowing gametes to be manipulated for specific purposes. As a result of the ability to control and manipulate cells easily, microfluidic devices have already been used for sperm behavior analyses,[4–6] sperm motility evaluation and selection,[7–12] cumulus removal,[13,14] fertilization[3,15] and embryo culture.[16–19]

As a 'lab-on-a-chip' technology, the ultimate goal of microfluidic IVF devices is to integrate all IVF procedures together. The integration of fertilization and embryo culture has been suggested,[20–24] but is yet to be realized, mainly due to the difficulties in medium exchange and washing without disturbing the gametes. Clark *et al.* and Suh *et al.* achieved microfluidic fertilization on gametes from pigs and mice, respectively, by designing narrowing paths in a straight microchannel which can park oocytes while allowing the passage of medium and sperm.[3,15] However, these devices are not convenient for medium changing, because they only permit very low flow speed, due to the restriction of the narrowing paths and the potential harm of fluidic shear stress on oocytes.

Microwell structures have already been used to trap single cells in microfluidic devices.[25] By minimizing the flow speed inside microwells, cells can be protected from fluidic shear stress,[26] and paracrine and/or autocrine factors produced by embryos which are believed to enhance their development[16] can also be preserved

[a]*Department of Biomedical Engineering, Tsinghua University School of Medicine, Beijing, 100084, China. E-mail: tshgl@mail.tsinghua.edu.cn; Fax: +86-10-62773059; Tel: +86-10-62772239*
[b]*National Engineering Research Center for Beijing Biochip Technology, 18 Life Science Parkway, Beijing, 102206, China*
[c]*Center of Reproduction Medicine, Department of Obstetrics and Gynecology, Third Hospital of Peking University, Beijing, 100191, China. E-mail: jie.qiao@263.net; Fax: +86-10-62013283; Tel: +86-10-82265080*
[d]*Shanxi Key Laboratory of Ecological Animal Science and Environmental Medicine, Shanxi Agricultural University, Taigu, Shanxi, 030801, China*

† Published as part of a LOC themed issue dedicated to Chinese Research: Guest Editor Professor Bingcheng Lin.

‡ Electronic supplementary information (ESI) available: Fig. S1, Fig. S2, Fig. S3, Movie S1. See DOI: 10.1039/c005296e

making a potentially preferable environment for cell culture. Heo and co-workers proposed an on-chip flow actuation system which can load and culture embryos in microwells without considering the fertilization process.[17] In addition, the microwell depth for effective oocyte/embryo entrapment was not suggested.

In this study, we used a microwell array to capture individual oocytes in the flow field, followed by *in situ* insemination, medium changing and embryo culture. Different microwell depths were designed and compared by finite element modeling and flow washing experiments, and the depth as high as 200 μm was found most effective in oocyte trapping and debris removal during the rapid *in situ* medium changing process, facilitating the integration of fertilization and embryo culture within a single microfluidic device. In addition, since each oocyte is lodged in an individual microwell, we can then for the first time track the entire fertilization and development process of any individual oocyte, providing convenience for the observation of embryo development and selection of healthy embryos for clinical use.

2 Materials and methods

2.1 Materials and reagents

Polydimethylsiloxane (PDMS, Sylgard 184) was supplied by Dow Corning Inc (Midland, MI). SU-8 photoresist was purchased from Microchem Inc (Newton, MA). Human tubal fluid (HTF) and potassium simplex optimized medium (KSOM) were purchased from Millipore (Temecula, CA). Pregnant mare's serum gonadotropin (PMSG) and human chorionic gonadotropin (hCG) were supplied by Hede Biotechnology (Beijing, China). Hyaluronidase, mineral oil and bisbenzimide (Hoechst 33342) were obtained from Sigma-Aldrich (St. Louis, MO).

2.2 Computational model

Microwell dimension is critical for reliable oocyte trapping and medium changing. Here we built finite element models (COMSOL 3.5, Comsol AB, Burlington, MA) and used 2D simulations to study the flow behavior in microwells with different depths. The model is based on the steady-state Navier–Stokes equation for an incompressible Newtonian fluid:

$$\rho(v\cdot\nabla)v = -\nabla p + \eta\nabla^2 v \quad (1)$$

where v is the velocity vector field, p is the pressure, ρ is the medium density, and η is the dynamic viscosity. The medium was modeled with a density of 1000 kg m^{-3} and a dynamic viscosity of 1 mPa·s, as in previous studies.[27] A uniform inlet velocity of 3 mm s^{-1} was used to simulate the experimental conditions. A zero pressure condition was applied to the outlet. No-slip boundary conditions were applied for the channel walls and microwell surfaces. Steady-state 2D velocity profiles and streamlines were plotted.

2.3 Device design and fabrication

The microfluidic device was designed based on the one used in our previous study.[14] The device consists of two PDMS layers, with a microchannel in the upper layer and a microwell array in the lower layer, as illustrated in Fig. 1(a) and (b). The microchannel is 1 mm in width and 200 μm in depth to transport sperm and oocytes, with a 10 mm long and 3 mm wide microchamber above the microwell array to receive all the oocytes in microwells, and the inlet (I1) and outlet (I2) are connected with the microchannel (Fig. 1(a)). Square-shaped microwells are 200 μm in width at a 50 μm interval, and each microwell row has a shift of 80 μm from its adjacent row to trap oocytes at different positions (Fig. 1(b), also see ESI, Fig. S1‡). Four microwell depths (50, 100, 150 and 200 μm) are designed on respective devices to compare their performance in oocyte entrapment and debris removal. During the experiment, oocytes are loaded into the microchannel, transported and lodged in the microwell array. Then sperm suspension is loaded, bringing motile sperm around the trapped oocytes to allow fertilization to occur, as illustrated in Fig. 1(c).

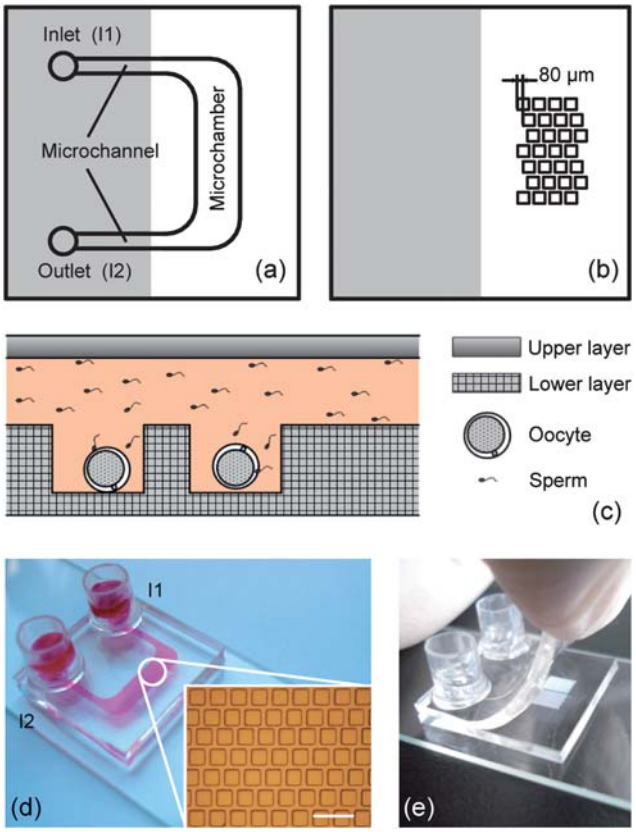

Fig. 1 The microwell-structured microfluidic device with two PDMS layers. (a) Illustration of the upper microchannel layer. The microchannel is 1 mm in width to transport sperm and oocytes, with a 3 mm wide microchamber to receive all the oocytes in the microwells. (b) Illustration of the lower microwell layer. Square-shaped microwells are 200 μm in width at a 50 μm interval, and each microwell row has a shift of 80 μm from its adjacent row to trap oocytes at different positions. The upper and lower layers are plasma bonded at the gray region. (c) Illustration of the cross section of the double-layer microfluidic device. (d) View of the microfluidic device fixed on a 76.2 mm × 25.4 mm microscopic slide, as well as the microwell array. The microchannel and the two reservoirs were filled with red dye. Scale bar is 500 μm. (e) View of the microfluidic device with the upper layer lifted.

The device was fabricated by following standard photolithography and micromolding procedures.[28] Briefly, SU-8 photoresist was patterned onto a 4 inch silicon wafer to form a master. Liquid PDMS prepolymer solution was poured onto

the master, cured at 70 °C for 1.5 h, and then peeled off the master, producing the final replica with the microstructures. The upper and lower layers were diced from the replica, treated in an oxygen plasma generator (FEMTO, Diener Plasma-Surface-Technology, Ebhausen, Germany), and irreversibly bonded together at the gray region shown in Fig. 1(a) and (b). The microchamber region was left unbonded so that the upper layer can be partially lifted for the retrieval of blastocysts. Two medium reservoirs were glued to the inlet and outlet on the upper layer with an epoxy structural adhesive (WD3620, Shanghai Kangda Chemical, Shanghai, China). An additional PDMS layer was molded on top of the glue to prevent the glue from contacting the culture medium. A view of the assembled device is shown in Fig. 1(d), and the device with the upper layer lifted is illustrated in Fig. 1(e).

2.4 Gametes collection

Sperm and oocytes were collected from 10-week and 8-week old Institute of Cancer Research (ICR) strain mice, respectively, by following standard procedures in accordance with institutional guidelines for care and use of animals. Briefly, female mice were intraperitoneally injected with 10 IU PMSG, and 10 IU hCG 48 h later. Fourteen hours following hCG injection, mice were sacrificed by cranial/cervical dislocation. Each oviduct was surgically removed, and the cumulus-oocyte masses were harvested into pre-equilibrated HTF drops then transported into 3 mg ml^{-1} hyaluronidase solution and denuded of cumulus cells. Males were sacrificed by cranial/cervical dislocation. Cauda epididymides and vasa deferentia were dissected out into a pre-equilibrated HTF drop, minced with ophthalmic scissors, then placed in a humidified 5% CO_2 incubator at 37 °C for 1 h for sperm to swim out and experience capacitation. Sperm concentration was assessed with a hemocytometer (Qiujing, Shanghai, China).

2.5 Oocyte trapping and debris removal tests

Microfluidic devices with 50, 100, 150 and 200 μm depths were tested for their effectiveness of oocyte entrapment and debris removal. In the oocyte entrapment test, microfluidic devices were pre-filled with HTF, then oocytes were loaded into microwells and rested for 2 min. A syringe pump (PHD 2000, Harvard Apparatus, Holliston, MA) was connected to reservoir I2 to generate a negative-pressure driven flow. The flow lasted for 2 min at each velocity, which kept increasing until an oocyte was washed out of its microwell. In the debris removal test, dead sperm samples were loaded into the devices and settled for 5 min. The flow was generated by the syringe pump and lasted for 2 min at each velocity. Images of microwells were captured before and after the flow using an inverted microscope (DM-IRB, Leica Microsystems GmbH, Wetzlar, Germany) under a 20× objective lens, and converted to binary images by MATLAB 7.1 (The Mathworks Inc, Natick, MA). The amount of debris was estimated by counting the number of black pixels (NBP) in these binary images, and the removal rate was calculated as the relative difference between the pre-flow NBP and post-flow NBP.

2.6 Fertilization and embryo culture

Each microfluidic device with 200 μm microwell depth was washed with ethanol, dried in a vacuum oven, treated in the plasma generator for hydrophilic surface modification, filled with HTF and placed in a 100 mm Petri dish with 15 ml distilled water to prevent evaporation of medium, followed by a 30 min UV exposure for sterilization. The devices were then equilibrated overnight in the humidified 5% CO_2 incubator at 37 °C. For the control group, 50 μl HTF and KSOM drops were prepared in 35-mm Petri dishes, covered by mineral oil, and equilibrated overnight in the incubator. All the HTF and KSOM used in the experiments were equilibrated overnight.

Denuded oocytes were loaded into reservoir I1 using a pipette (Eppendorf, Hamburg, Germany), and a gravity-driven flow from I1 to I2 was generated to guide oocytes into the microwell array area. By adjusting the flow using the pipette, each oocyte was individually aligned above a single microwell and then sank into the well by gravity. Sperm were then added into I1 and transported by the gravity-driven flow into the microchamber. For the control group, oocytes and sperm were sequentially added into the oil-covered HTF drops in Petri dishes. Microfluidic devices and Petri dishes were then placed back in the humidified 5% CO_2 incubator at 37 °C. The final sperm concentration was adjusted to $\sim 1 \times 10^6$ sperm ml^{-1} in both the microchannels and the oil covered drops.

After incubation for 8 h, I1 and I2 reservoirs were depleted, and KSOM was added into I1, generating a flow speed in the range of 2–5 mm s^{-1} to substitute all the HTF in the microchannels while removing the debris. Substituted medium was depleted from I2. For the control group, oocytes were washed in KSOM drops three times, and transferred to a KSOM embryo culture drop. Fertilization was determined by the occurrence of two pronuclei, which was assessed after 9 h incubation. Embryo development status was examined and individually tracked after 24, 48, 72 and 96 h incubation. Each phase contrast image was taken by using the DM-IRB microscope under 20× objective lens. Data derived from microwells and conventional oil-covered drops in Petri dishes were statistically compared using Student *t*-test, where $P < 0.05$ was considered significantly different.

Blastocysts were individually retrieved from the microwells after 104 h incubation with the following steps (see ESI, Fig. S2‡). Under microscopic observation, a pipette is aligned above a trapped blastocyst, and pressed down towards the sidewall of the microwell, which deforms due to the elastic nature of PDMS. The blastocyst is then retrieved from the microwell by the flow generated by pipetting. The retrieved blastocysts were transported into 10 μg ml^{-1} Hoechst 33342 staining solution and incubated at 37 °C, 5% CO_2 for 30 min. The stained blastocysts were then mounted on a glass slide with a cover slip on top. Fluorescent images were captured using the DM-IRB microscope under 40× objective lens. The excitation and emission spectra wavelengths for Hoechst 33342 are 346 nm and 460 nm respectively.

3 Results

3.1 Computational analysis for different microwell depths

Fig. 2(a) and (b) illustrates the velocity contours and streamlines of four microwells with different depths (50, 100, 150 and

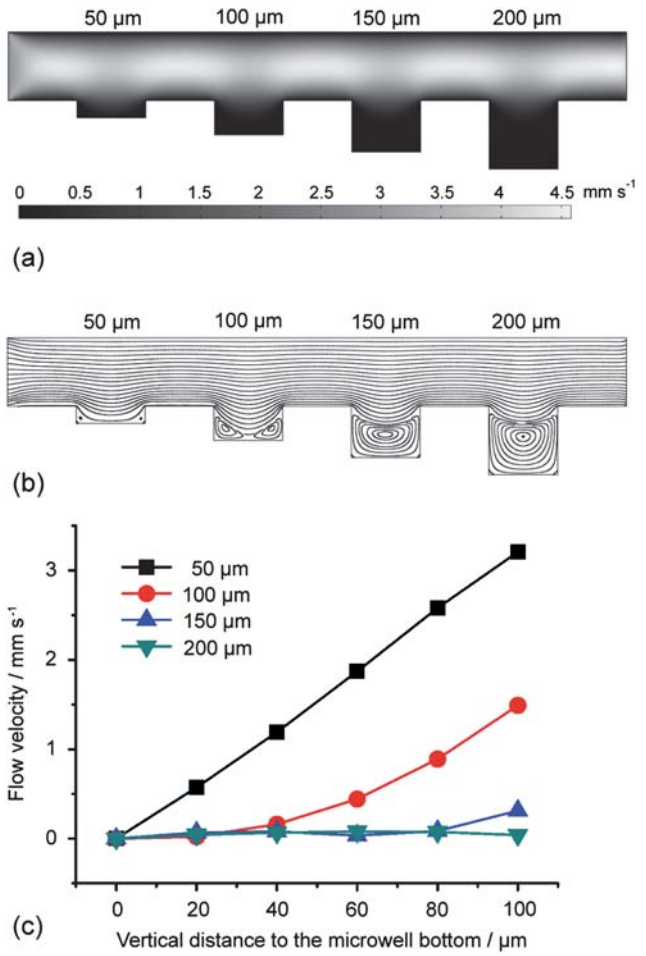

Fig. 2 Computational analysis of microwells with different depths. (a) Velocity contours for microwells with different depths. (b) Streamlines for microwells with different depths. (c) Velocity at the microwell horizontal slice center as a function of its vertical distance to the bottom.

200 μm) in a 200 μm deep microchannel. Medium flows from left to right with an inlet velocity of 3 mm s^{-1}, comparable to the experimental conditions. As shown in Fig. 2(a), the flow velocity is higher in shallow wells (50 and 100 μm) than in deep ones (150 and 200 μm), making it more difficult for shallow wells to hold oocytes. As observed in the streamline analysis (Fig. 2(b)), eddies are formed in the corners for shallow wells (50 and 100 μm) but enlarge and occupy the entire wells for deep ones (150 and 200 μm). Fig. 2(c) represents the flow velocity at the horizontal slice center of a microwell as a function of the vertical distance to the microwell bottom. The distance ranges from 0 to 100 μm, since a normal mouse oocyte has a diameter close to 100 μm. Compared to the inlet velocity (3 mm s^{-1}), the maximum flow velocity around a trapped oocyte is reduced by 50%, 90% and 97% for the 100, 150 and 200 μm depths respectively, but not significantly changed for the 50 μm depth.

3.2 Oocyte trapping and debris removal tests for different microwell depths

In the oocyte trapping test, the flow speed kept increasing until the oocyte was washed out. The increasing step was 0.02 mm s^{-1} for the 50 μm depth, 0.05 mm s^{-1} for the 100 μm depth, 0.5 mm s^{-1} for the 150 μm depth and 1 mm s^{-1} for the 200 μm depth. Five replications were made, and the oocyte washing out velocities for these four depths are 0.128 ± 0.011, 0.500 ± 0.035, 5.10 ± 0.42 and 15.4 ± 0.9 mm s^{-1}, respectively, as illustrated in Fig. 3(a). Since the flow speed in our medium changing process is normally larger than 1 mm s^{-1}, the 50 and 100 μm depths are not suitable for use.

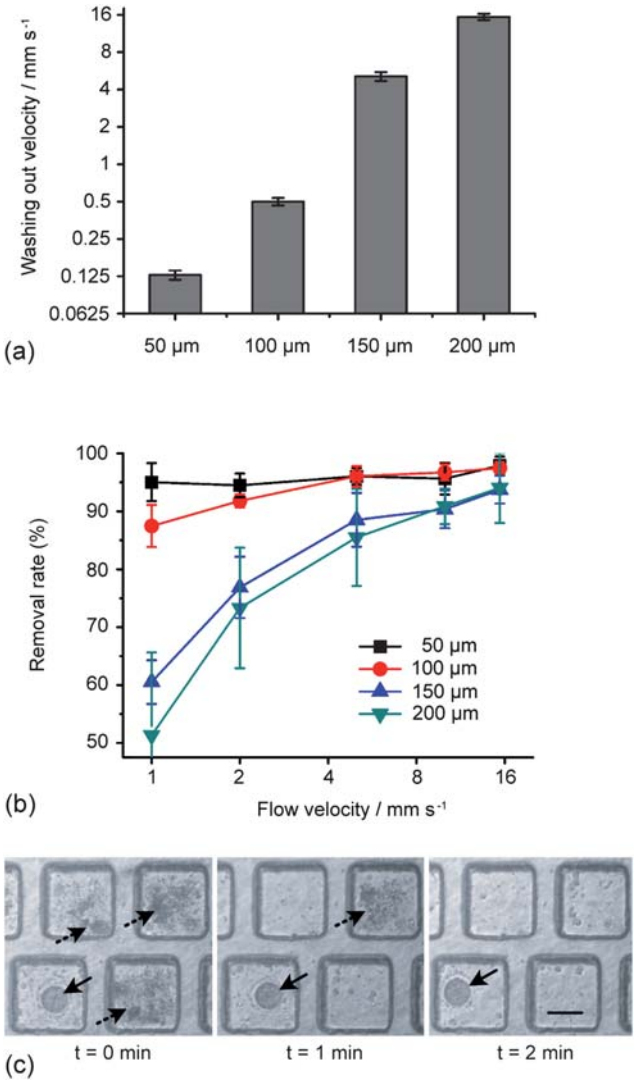

Fig. 3 Oocyte trapping and debris removal tests. (a) The oocyte washing out velocity for different microwell depths. The trapped oocytes were washed out at 0.128 ± 0.011, 0.500 ± 0.035, 5.10 ± 0.42 and 15.4 ± 0.9 mm s^{-1} for the 50, 100, 150 and 200 μm depths, respectively. The velocity is plotted on a logarithmic scale. (b) The debris removal rate for the microwells as a function of flow velocity ranging from 1 mm s^{-1} to 15.4 mm s^{-1}. The velocity is plotted on a logarithmic scale. (c) Demonstration of the medium changing process in the 200 μm deep microwells at the speed of 3 mm s^{-1}. An oocyte (solid arrow) was already trapped in a microwell. Before medium changing, microwells were filled with debris (dashed arrow). After washing for 1 min, part of the debris was washed out by the eddies formed in the microwells. After 2 min, most of the debris was removed. Scale bar is 100 μm.

In the debris removal test, flow velocities of 1, 2, 5, 10 and 15.4 mm s^{-1} were applied to the devices with the four depths. We examined six microwells for each depth, and the relationship between the removal rate and flow speed is illustrated in Fig. 3(b). The 150 and 200 μm depths have similar debris removal performance, with 70%+ debris removed at 2 mm s^{-1} and 80%+ at 5 mm s^{-1}. However, according to Fig. 3(a), the 150 μm depth can no longer hold oocytes when the flow speed increased to 5 mm s^{-1}, and is therefore not able to support oocyte/debris separation at high flow speed. Consequently, we finally selected the 200 μm depth for our IVF experiments.

To confirm that the 200 μm deep microwell is able to clean the debris while holding the oocytes during medium changing, a microfluidic device containing both oocytes and sperm debris after 9 h insemination was examined. The syringe pump was connected to reservoir I2 to generate a flow speed of 3 mm s^{-1}. The medium substitution process also lasted for 2 min, which is approximately the time taken in our microfluidic IVF experiments, and is faster than the standard Petri dish IVF (normally ~5 min in our hands, depending on the operator's skill and the number of oocytes). Fig. 3(c) illustrates the medium changing process. Before medium changing (0 min), microwells were filled with debris (dashed arrow). After washing for 1 min, debris was partially removed. Meanwhile, the trapped oocyte (solid arrow) rotated in the microwell, demonstrating the existence of eddies predicted by our previous simulation (see ESI, Movie S1‡). After 2 min, most of the debris was swept out, with the oocyte still resting in the microwell.

3.3 *In vitro* fertilization

The experiments were independently repeated four times. At 9 h post-insemination, similar fertilization rates were obtained between microwells (69.0 ± 6.1%, $N = 64$) and controls (71.4 ± 12.3%, $N = 109$) without significant difference ($P > 0.1$), as shown in Fig. 4.

3.4 Embryo culture and single embryo development tracking

After medium exchange, embryo development was observed and recorded. Among all the zygotes, the percentages of two-cell, four-cell, morula and blastocyst stage embryos after 24, 48, 72 and 96 h of incubation were recorded and calculated, respectively, as illustrated in Table 1. No significant differences ($P > 0.1$) were observed between the two groups in each development stage.

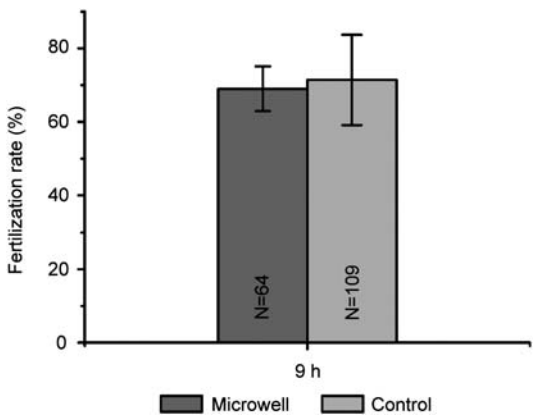

Fig. 4 Fertilization rates of oocytes from microwell IVF and control Petri dish IVF.

Since each zygote was lodged in a particular microwell, the fertilization and development status of each oocyte can be tracked individually. Fig. 5(a) illustrates the development tracking process of a normal zygote. Two pronuclei appeared at 9 h post-insemination, and two-cell, four-cell, morula and blastocyst stages were observed at 24, 48, 72 and 96 h, respectively. The blastocyst was then retrieved and stained by Hoechst 33342 at 104 h, shown in Fig. 5(b). Abnormal development can also be discerned and studied. As shown in Fig. 5(c), an oocyte attacked by many sperm at 9 h fractured at 24 h.

4 Discussion

In this study, we have proposed a microfluidic oocyte trapping method which supports rapid medium exchange, and demonstrated the integration of fertilization and embryo culture. A microwell-structured device was designed, and microwells with 50, 100, 150 and 200 μm depths were studied and compared for their performance on oocyte trapping and debris removal, based on both computational simulation methods and flow washing experiments. The 3 mm wide and 200 μm high microchamber above the microwell array ensures the uniformity of flow rates for microwells in different positions (see ESI, Fig. S3‡). According to the simulation, the maximum flow velocity near a trapped oocyte is reduced by 0, 50, 90 and 97% for the four microwell depths, respectively, compared to the inlet, suggesting that it is more difficult for the oocytes to exit deeper microwells. This is consistent with the observed oocyte washing out velocities for the four depths, which are 0.128, 0.500, 5.10 and 15.4 mm s^{-1}. The 50 and 100 μm depths allow only very low washing-out velocities, and are not capable of holding oocytes against flow fluctuations occurred during sperm loading and medium perfusion. For the medium exchange velocity in the range of 2–5 mm s^{-1}, both the 150 and 200 μm depths are able to remove over 70%–80% debris. However, the 150 μm deep microwell fails to hold the oocyte at the flow speed of 5 mm s^{-1}, while the 200 μm deep microwell has a much higher threshold of 15.4 mm s^{-1}. As a result, the 200 μm deep microwell surpasses the other three depths in the effectiveness of oocyte trapping and debris removal, and was therefore selected for our IVF experiments.

The microwell width is 200 μm throughout the device to accommodate the dimension of oocytes and embryos. A murine oocyte is ~100 μm in diameter and a hatched blastocyst may expand to more than 150 μm, so the dimension of the microwell could provide enough space for embryo development. During

Table 1 Embryo development comparison between microwell IVF and control Petri dish IVF

	Microwell IVF rate (%)	Control IVF rate (%)
Two-cell (24 h)	96.9 ± 6.3	96.4 ± 4.2
Four-cell (48 h)	92.7 ± 6.3	91.7 ± 6.4
Morula (72 h)	93.8 ± 7.2	92.7 ± 6.7
Blastocyst (96 h)	87.5 ± 10.2	87.8 ± 8.2

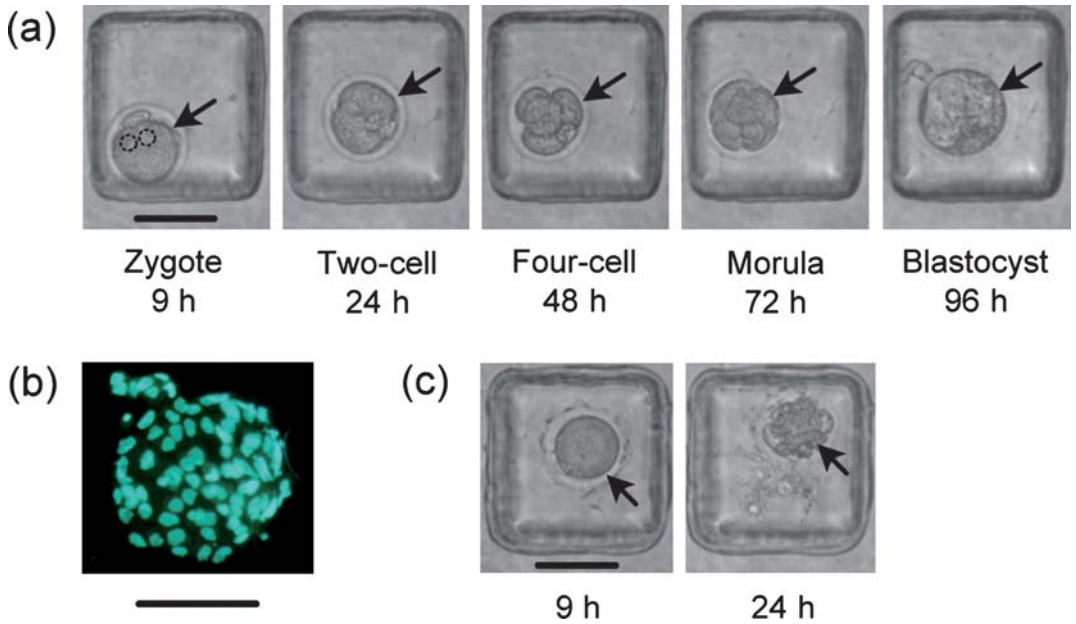

Fig. 5 Single embryo development tracking. Scale bars are 100 μm. (a) Normal development of a zygote (arrow). Two pronuclei in the zygote were marked by dashed circles. (b) Fluorescent image of the retrieved blastocyst in (a). (c) An oocyte (arrow) attacked by many sperm at 9 h fractured at 24 h.

oocyte trapping, it takes only a few seconds for an oocyte to sink into a microwell by gravity. Oocyte trapping and debris removal tests were performed under continuous flow generated by using a syringe pump. To save manipulation time, we used a pipette instead in our IVF experiments to exchange medium, resulting in a fluctuation in the flow speed from 2 to 5 mm s^{-1}. Since the effectiveness of the 200 μm deep microwell has already been proven within this range, the device can still produce satisfactory oocyte trapping and debris removal results. Our microwell design overcomes the medium changing problem faced by previous microfluidic IVF devices,[3,15] and hence facilitates the integration of fertilization and embryo culture.

We used a standard sperm concentration of $\sim 1 \times 10^6$ sperm ml^{-1} in both our microfluidic device and conventional Petri dishes. Suh *et al.* claimed that they needed a lower sperm concentration ($2–8 \times 10^4$ sperm ml^{-1}) in microchannels to improve fertilization outcome,[3] possibly because their device exposed oocytes directly in the course of sperm so that more sperm encountered oocytes. In contrast, in our design, the microwells shield the oocytes from the sperm flow, preventing them from encountering too many sperm. Therefore, the $\sim 1 \times 10^6$ sperm ml^{-1} concentration led to satisfactory rates of fertilization in our devices.

During insemination, rotation and movement of oocytes can be observed immediately after sperm attachment, as discussed in previous studies.[29] This phenomenon makes it difficult for conventional methods to allocate oocytes in one place and track their fertilization and development status individually. In contrast, it has been made possible for our device to confine oocyte movement within a square-shaped microwell. Microwell depth is critical for effective confinement. Sperm–oocyte clusters were observed to exit from the 50, 100 and 150 μm deep wells, however, this phenomenon was not observed when the depth of the microwell increased to 200 μm.

Currently, microfluidic systems have been reported to perform embryo culture in both static and dynamic conditions. For the static systems, embryos were parked in straight channels[16] or microchambers[19] and cultured without moving the medium. For the dynamic systems, embryos experienced changing medium environment[20] or constant stimulation[18] during their development. Those static systems tend to produce higher blastocyst rates.[16,19] We therefore choose to culture our embryos under static culture conditions to allow for the direct comparison with the control, *i.e.*, oil-covered drops in Petri dishes. However, the *in vivo* embryo culture environment in Fallopian tubes is quite dynamic, providing renewing medium for embryos. In addition, exposure to appropriate flow stress and mechanical stimulation during embryo development is believed to mimic the *in vivo* conditions and may further enhance the *in vitro* culture outcome,[18] which will also be taken into account in our future study.

After *in vitro* embryo culture, blastocysts need to be collected and transferred back to the uterus. However, the embryo retrieval step is not convenient for the reported microfluidic IVF and embryo culture devices, for they had to generate a backward flow to make embryos return to the inlet.[3,15,16] Whereas with our device, the PDMS layers are partially bonded and the microchannel layer can be lifted while each embryo is still trapped in the microwell layer at its fixed position. This feature allowed us to directly remove embryos from the microwells by pipetting with the retrieval rate close to 100%.

5 Conclusion

IVF is a crucial therapy to treat human infertility. In this work, we developed a microwell array structured microfluidic device to simplify the medium changing process in IVF, and achieved the integration of single oocyte trapping, fertilization and embryo

culture within a microfluidic device. Embryos can be individually monitored and tracked in our devices during their development, and conveniently retrieved afterwards. These results demonstrate the great potential for a microfluidic lab on a chip system being a powerful tool towards integration and automation in reproductive science research and clinical applications.

Acknowledgements

This work was supported by the grant of National High-Tech Program (2006AA020701).

References

1 P. C. Steptoe and R. G. Edwards, *Lancet*, 1978, **312**, 366.
2 A. Nagy, M. Gertsenstein, K. Vintersten and R. Behringer, in *Manipulating the mouse embryo: a laboratory manual*, Cold Spring Harbor Laboratory Press, Cold Spring Harbor, 3rd edn, 2003, ch. 14, pp. 576–579.
3 R. S. Suh, X. Y. Zhu, N. Phadke, D. A. Ohl, S. Takayama and G. D. Smith, *Hum. Reprod.*, 2006, **21**, 477–483.
4 L. J. Kricka, O. Nozaki, S. Heyner, W. T. Garside and P. Wilding, *Clin. Chem.*, 1993, **39**, 1944–1947.
5 S. Koyama, D. Amarie, H. A. Soini, M. V. Novotny and S. C. Jacobson, *Anal. Chem.*, 2006, **78**, 3354–3359.
6 M. D. C. Lopez-Garcia, R. L. Monson, K. Haubert, M. B. Wheeler and D. J. Beebe, *Biomed. Microdevices*, 2008, **10**, 709–718.
7 L. J. Kricka, X. Y. Ji, O. Nozaki, S. Heyner, W. T. Garside and P. Wilding, *Clin. Chem.*, 1994, **40**, 1823–1824.
8 L. J. Kricka, I. Faro, S. Heyner, W. T. Garside, G. Fitzpatrick, G. McKinnon, J. Ho and P. Wilding, *J. Pharm. Biomed. Anal.*, 1997, **15**, 1443–1447.
9 B. S. Cho, T. G. Schuster, X. Y. Zhu, D. Chang, G. D. Smith and S. Takayama, *Anal. Chem.*, 2003, **75**, 1671–1675.
10 T. G. Schuster, B. Cho, L. M. Keller, S. Takayama and G. D. Smith, *Reprod. BioMed. Online*, 2003, **7**, 75–81.
11 M. C. McCormack, S. McCallum and B. Behr, *J. Urol.*, 2006, **175**, 2223–2227.
12 J. M. Wu, Y. Chung, K. J. Belford, G. D. Smith, S. Takayama and J. Lahann, *Biomed. Microdevices*, 2006, **8**, 99–107.
13 H. C. Zeringue, J. J. Rutledge and D. J. Beebe, *Lab Chip*, 2005, **5**, 86–90.
14 C. Han, R. Ma, Z. Sun, Z. Yu, G. Huang, Y. Zhou, J. Qiao, J. Wang and J. Cheng, *Proceedings of the 13th International Conference on Miniaturized Systems for Chemistry and Life Sciences*, Jeju, 2009.
15 S. G. Clark, K. Haubert, D. J. Beebe, C. E. Ferguson and M. B. Wheeler, *Lab Chip*, 2005, **5**, 1229–1232.
16 S. Raty, E. M. Walters, J. Davis, H. Zeringue, D. J. Beebe, S. L. Rodriguez-Zas and M. B. Wheeler, *Lab Chip*, 2004, **4**, 186–190.
17 Y. S. Heo, L. M. Cabrera, J. W. Song, N. Futai, Y. C. Tung, G. D. Smith and S. Takayama, *Anal. Chem.*, 2007, **79**, 1126–1134.
18 M. S. Kim, C. Y. Bae, G. Wee, Y. M. Han and J. K. Park, *Electrophoresis*, 2009, **30**, 3276–3282.
19 J. Melin, A. Lee, K. Foygel, D. E. Leong, S. R. Quake and M. W. M. Yao, *Dev. Dyn.*, 2009, **238**, 950–955.
20 R. S. Suh, N. Phadke, D. A. Ohl, S. Takayama and G. D. Smith, *Hum. Reprod. Update*, 2003, **9**, 451–461.
21 M. B. Wheeler, E. M. Walters and D. J. Beebe, *Theriogenology*, 2007, **68**, S178–S189.
22 G. D. Smith and S. Takayama, *Theriogenology*, 2007, **68**, S190–S195.
23 S. G. Clark, E. M. Walters, D. J. Beebe and M. B. Wheeler, *Theriogenology*, 2003, **59**, 441.
24 J. Mizuno, S. Ostrovidov, H. Nakamura, K. Akaishi, H. Inui, Y. Sakai, T. Fujii, K. Anzai and A. Watanabe, *Hum. Reprod.*, 2007, **22**, I169–I170.
25 J. R. Rettig and A. Folch, *Anal. Chem.*, 2005, **77**, 5628–5634.
26 N. Korin, A. Bransky, M. Khoury, U. Dinnar and S. Levenberg, *Biotechnol. Bioeng.*, 2009, **102**, 1222–1230.
27 A. Manbachi, S. Shrivastava, M. Cioffi, B. G. Chung, M. Moretti, U. Demirci, M. Yliperttula and A. Khademhosseini, *Lab Chip*, 2008, **8**, 747–754.
28 D. C. Duffy, J. C. McDonald, O. J. A. Schueller and G. M. Whitesides, *Anal. Chem.*, 1998, **70**, 4974–4984.
29 A. Nir, *J. Theor. Biol.*, 2002, **214**, 171–179.

